Generator Motoring Protection – Are You Protected?

Dale Finney, Michael Thompson, Normann Fischer, and Amandeep Kalra,
Schweitzer Engineering Laboratories, Inc.

***Abstract*—Steam turbines can be damaged upon loss of steam flow while the generator remains connected to the power system. Reverse power relays are used to detect the motoring power into the electrical machine and open the generator main breaker to prevent damage from this abnormal operating condition. The motoring power for large steam turbines can be a very small fraction of the power rating, leading to sensitivity issues and a failure to detect and trip for this condition. Reverse power protection systems that have been proven to work dependably over many normal shutdowns may not provide the expected protection during an inadvertent motoring event.**

During normal sequential trip shutdown sequences, the active and reactive power outputs are ramped down to zero prior to tripping the turbine. In this case, the power factor is near unity and the relay has little difficulty measuring the active power component of the signal. However, during a true inadvertent motoring event, the reactive power output may remain at near pre-event levels, resulting in a significant MVA output at near-zero power factor. During these conditions, small angle errors in the instrument transformers and measuring devices can result in large errors in measuring the very small active component of the apparent power flow.

This paper discusses motoring events and the resulting active and reactive power flows. It reviews current transformer (CT) and voltage transformer (VT) accuracy as defined by ANSI IEEE C57.13 and IEC 61869. It examines existing reverse power relays used for generator protection and presents a new algorithm for dependable motoring detection. It also describes the implementation and testing of the algorithm on an embedded processing platform.

I. Introduction

This paper provides insight into the challenge of dependably detecting a motoring event on a large synchronous generator. It is an expansion of [1] and provides updated and additional material.

When a generator loses its prime mover while connected to the power system, it begins to draw power from the network to supply its losses. This condition does not present a risk to the generator; however, there is a risk of damage to the prime mover. The amount of power drawn (motoring power) depends on the machine type. Motoring power is often expressed as a percentage of rated power. The motoring power of reciprocating engines and combustion turbines is relatively high. The motoring power of a hydroelectric generator is high or low, depending on whether the tail race water level is above or below the turbine blades. Motoring power can be 0.2 to 2 percent for the latter case. A steam turbine that motors under full vacuum also presents a very low motoring power of 0.5 to 3 percent.

Microprocessor-based relays are now commonly applied for generator protection. Often, the same current transformer (CT) is used both for reverse power detection and for the remainder of the generator protection functions. The minimum current detection requirement can be very low. For example, assuming that the CT primary is 120 percent of the generator-rated current, that the generator voltage is 105 percent of the rated voltage, and that the generator is motoring at 0.5 percent at unity power factor, the current seen by the relay is 0.33 percent of its nominal rating. For a 1 A nominal rated CT, the relay must accurately measure a current of only 3.3 mA. In order to provide a margin for error, the element pickup is typically set at 50 percent of the expected motoring power [2]. Often, the actual motoring power is measured during the initial start-up commissioning procedures and adjusted accordingly.

The dynamic range for protection functions in a generator application is quite large. Motoring elements (32) may require accurate measurement at a low fraction of a percentage of the CT nominal rating, as described previously, while fault protective elements (87, 21, and so on) may require accurate measurement at ten to twenty times the CT nominal rating. Before multifunction protection systems entered common usage, this issue was sometimes addressed by using metering accuracy instrument transformers for the reverse power elements and relay accuracy instrument transformers for the fault protective elements. Luckily, numerical technology can use advanced algorithms to address this seemingly impossible demand on instrument transformer and relay accuracy.

For a motoring event with the machine operating at unity power factor, the magnitude of the current can be very low. Generator relays are designed to measure this low current value. Small angle measurement errors are not a problem. However, if the expected motoring power is very low and the generator also produces a significant reactive power, an angle error can result in a loss of dependability [2] [3] [4]. This is illustrated in Fig. 1, where an angle error can shift the measured power to the point shown by the red triangle.

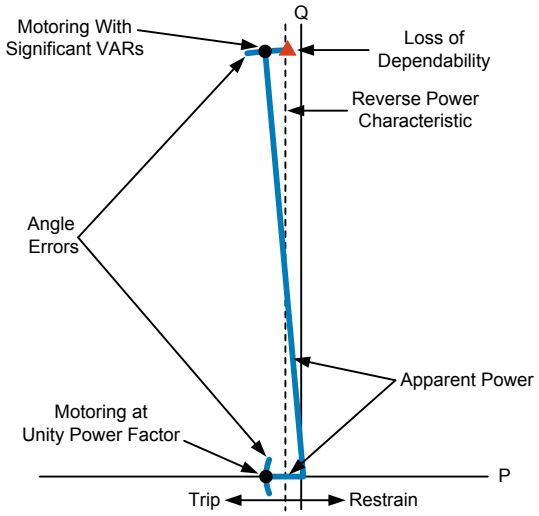

Fig. 1. Angle Error Impact During Motoring

A modern microprocessor-based design can have very good angle accuracy. This is mainly due to factory calibration. Fig. 2 shows the variation of measured active power error as a function of power factor. This plot was generated by fixing the active power at 0.5 percent and varying the reactive power from 0 to 50 percent. The test was carried out by secondary injection at the relay terminals after normal factory calibration.

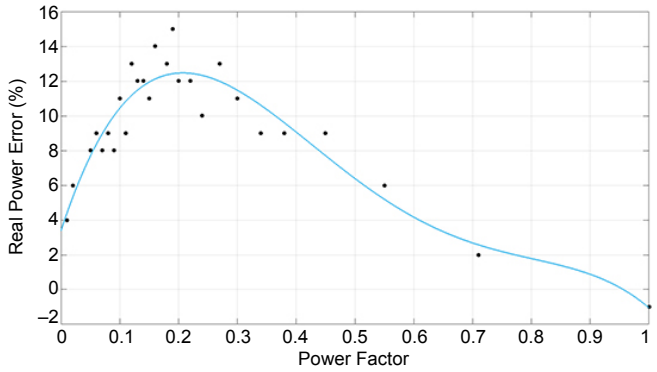

Fig. 2. Typical Relay Active Power Error as Function of Power Factor

We may apply the following analysis to estimate the total tolerable angle error. If we assume that the generator operates initially at rated MVA with a power factor of 0.85 and that the reactive power remains constant during a motoring event, the reactive power Q_M is as shown in (1).

$$Q_M = \sqrt{1-0.85^2} = 0.527 \tag{1}$$

Assuming a motoring power P_M of 0.5 percent, we obtain (2).

$$\theta_M = \tan^{-1}\left(\frac{0.527}{0.005}\right) = 89.456 \text{ degrees} \tag{2}$$

Assuming a reverse power pickup setting of 0.5 P_M results in (3) and (4).

$$\theta'_M \approx \tan^{-1}\left(\frac{0.527}{0.0025}\right) = 89.728 \text{ degrees} \tag{3}$$

$$\theta_{ERR} = \theta'_M - \theta_M = 0.27 \text{ degrees} = 16 \text{ minutes} \tag{4}$$

We conclude that a loss of dependability can occur for a total angle error as minor as 0.25 degrees and that some installations may be vulnerable to poor dependability during an inadvertent motoring event. Because the relay is usually calibrated to minimize internal sources of angle error, the primary source resides with the instrument transformers; i.e., CTs and voltage transformers (VTs).

While inadvertent motoring events are rare, there have been incidents of failures to trip. These require operator intervention to separate the generator from the power system. Reverse power protection systems that have been proven to work dependably over many normal shutdowns may not provide the expected protection during an inadvertent motoring event.

Because the greatest source of error is the instrument transformers, the angle error tolerances as defined by the American National Standards Institute (ANSI) Institution of Electrical and Electronics Engineers (IEEE) and the International Electrotechnical Commission (IEC) are reviewed in this paper to provide context for the error tolerance calculated in (1) through (4).

II. Generator Response During a Motoring Event

Typically, when the generator is connected to the power system, the automatic voltage regulator (AVR) is configured to maintain rated voltage at its terminals. Limiters in the AVR ensure that the reactive power produced by the machine remains within the generator's capability curve as shown in Fig. 3.

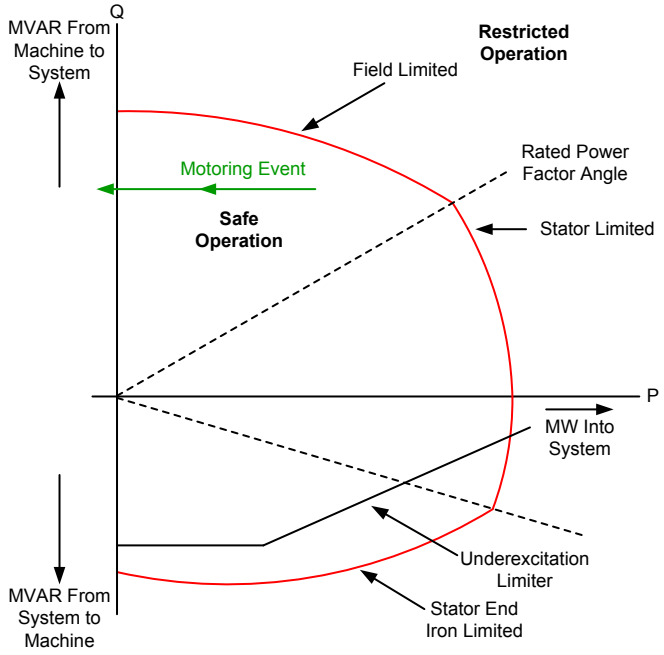

Fig. 3. Inadvertent Motoring Event Superimposed on Generator Capability Curve

During a controlled shutdown of the generator, the AVR is usually switched to operate at unity power factor. During a controlled shutdown and for certain abnormal operating condition (nonfault) trips, the generator is often allowed to intentionally motor to avoid overspeed when the generator breaker opens. The reverse power relay is used to confirm that the steam valves are fully closed and seated and that there is no steam flow that can cause the turbine to speed out of control once the generator is no longer locked to the synchronous speed determined by the system frequency. This process is known as sequential tripping. The AVR should also be switched to unity power factor operation during sequential tripping to ensure dependable operation of the reverse power element.

During an unintentional motoring event, if the AVR continues to regulate the generator terminal voltage, the reactive power can be significant and the generator active and reactive power outputs follow the path shown in green in Fig. 3 (labeled "Motoring Event"). This is the scenario in which dependability may be lost.

The response shown in Fig. 3 is a simple approximation that does not consider the impact of load angle or AVR response on the reactive power output. We can investigate the validity of this approximation as follows.

The machine active power (P) and reactive power (Q) are given in the complex power equation (5).

$$P + jQ = \frac{E \bullet V}{X}\sin\delta + j\left(\frac{E \bullet V}{X}\cos\delta - \frac{V^2}{X}\right) \quad (5)$$

In (5), E is the internal voltage magnitude, V is the terminal voltage magnitude, X is the generator reactance, and δ is the load angle. When motoring occurs, δ approaches zero. From (5), we note that P and Q are both affected. This, in turn, affects the terminal voltage. The AVR reacts to bring the voltage back to nominal, causing a further change in Q. The final value for Q depends on the details of the system.

Fig. 4 shows a simulated response of a machine to a motoring event (AVR in automatic mode). The oscillations at the beginning of the plot are due to initialization errors of the model. A reverse power event is simulated at 3 seconds by reducing the generator mechanical power input. Note that the terminal voltage undergoes a very slight increase and the reactive power undergoes a slight decrease. This simulated response confirms the validity of the response shown in Fig. 2.

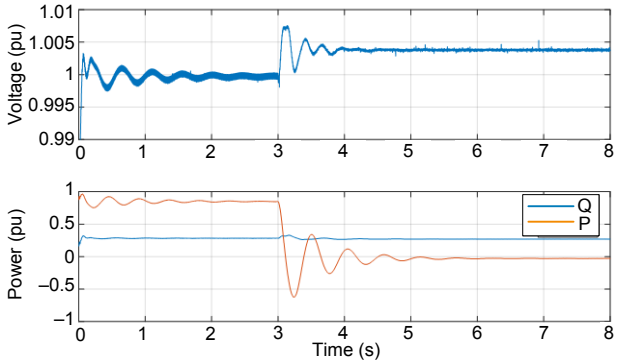

Fig. 4. Simulated Motoring Response

III. Instrument Transformer Accuracy

A. Nature of Instrument Transformer Errors

In order to evaluate the possibility that the element dependability may be compromised, it is necessary to understand the nature of the instrument transformer errors. In general, a CT or VT may be represented by the equivalent circuit in Fig. 5. The complex impedances $Z_P = R_P + jX_P$ and $Z_S = R_S + jX_S$ represent the resistance and leakage reactance of the primary and secondary windings. In this equivalent circuit, the primary impedance is reflected to the secondary side by the square of the turns ratio. The parallel branch of the circuit, which includes R_E and jX_M, represents the magnetizing branch impedance. Z_B is the connected burden, which includes secondary wiring, relays, and meters. The exciting current I_E in the magnetizing branch is a nonlinear function of the saturation voltage E_S and is defined by the excitation curve.

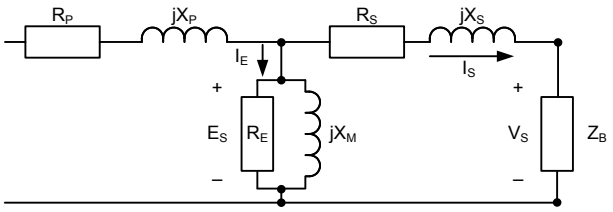

Fig. 5. Instrument Transformer Equivalent Circuit

In the case of a CT, the input to the circuit is an ideal current source with a value of I_P/CTR where I_P is the primary current and CTR is the CT ratio. For protection, the range of interest for the current is 0 to 20 times the rated current. In a protection-class CT (for example, ANSI Classes C and K), the primary impedance and secondary leakage reactance can be neglected. Fig. 6 shows the relationship between the primary, secondary, and excitation currents.

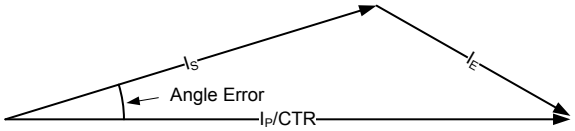

Fig. 6. CT Relationships

In the case of a VT, the input to the circuit is an ideal voltage source with a value of V_P/VTR where V_P is the primary voltage and VTR is the VT ratio. The range of interest for the voltage is 90 to 110 percent of the rated voltage. The primary source of error (ΔV) is the voltage drop across the winding impedance branches as shown in Fig. 7. It can be approximated using (6).

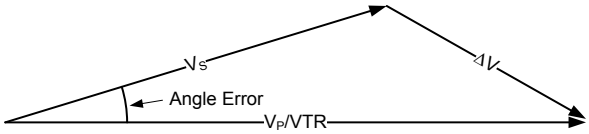

Fig. 7. VT Relationships

$$\Delta V \approx \frac{V_P}{VTR} \bullet \frac{Z_P + Z_S}{Z_P + Z_S + Z_B} \quad (6)$$

An examination of the industry standards for instrument transformers that are used for protection and metering reveals that errors greater than 0.25 degrees (15 minutes) can be expected in real-world applications. Subsections 1 and 2 summarize the relevant specifications.

1) ANSI IEEE Accuracy Specifications

For CTs, IEEE C57.13 Standard Requirements for Instrument Transformers specifies three metering accuracy classes (0.3, 0.6, and 1.2) and five standard burdens (0.1, 0.2, 0.5, 0.9, and 1.8 ohms) [5]. These specifications are given for a CT nominal secondary of 5 A and a frequency of 60 Hz. The standard burdens are inductive at a power factor of 0.9. For example, a CT with a metering accuracy of 0.3B-0.5 has an accuracy class of 0.3 when connected to an impedance of 0.45 + j0.22 ohms. If the nominal secondary current is a value other than 5 A, the impedance is multiplied by (5/nominal secondary)^2.

The limits for angle errors at the standard burden are given in Fig. 8 and Fig. 9. In these figures, the ordinate axis is the ratio correction factor, which is a measure of the total error including both magnitude and angle errors. Note that the angle error limit for CTs depends on the accuracy class as well as the current magnitude.

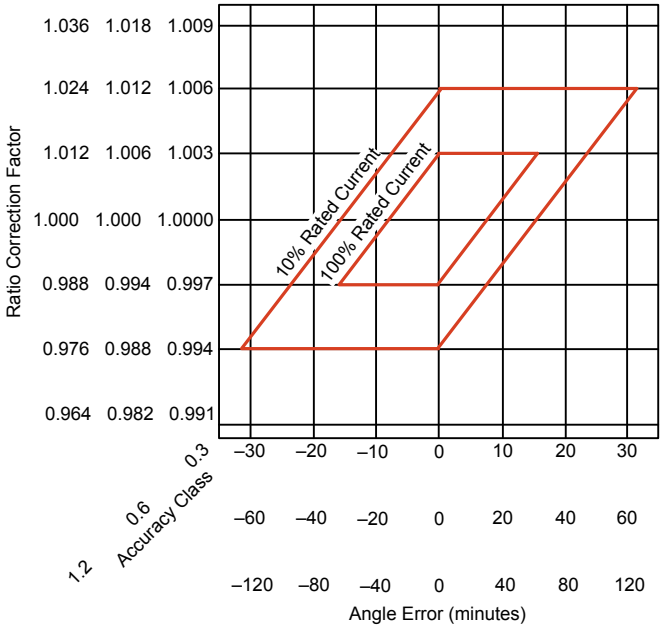

Fig. 8. Metering CT Angle Error Limits (IEEE C57.13)

IEEE C57.13 does not specify an angle error limit for the protection accuracy class. However, the CT may be dual-rated. In this case, the CT nameplate lists a metering accuracy and a protection accuracy. If the CT only has a protection accuracy class, then there is no limit requirement for angle error.

IEEE C57.13 also defines three metering accuracy classes for VTs (0.3, 0.6, and 1.2) and six standard burdens. Table I lists the burdens and their associated power factors.

TABLE I
VT STANDARD BURDENS (IEEE C57.13)

Designation	Burden (VA)	Power Factor
W	12.5	0.10
X	25	0.70
M	35	0.20
Y	75	0.85
Z	200	0.85
ZZ	400	0.85

Fig. 9 shows the angle error limits for VTs at the standard burdens. The VT must meet these limits for voltages between 90 to 110 percent of the rated voltage.

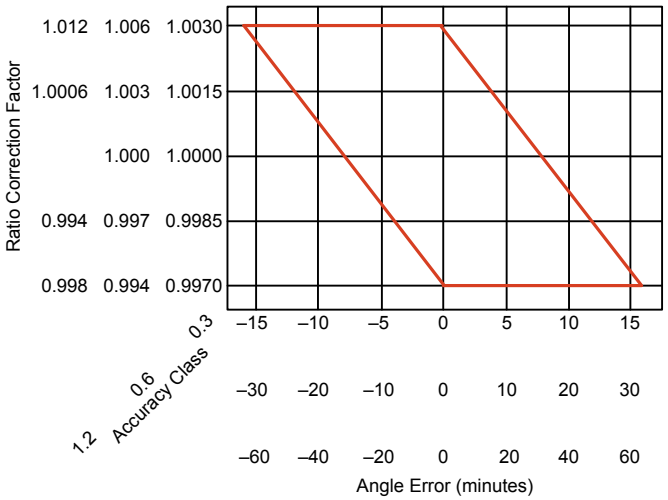

Fig. 9. Metering VT Angle Error Limits (IEEE C57.13)

2) IEC Accuracy Specifications

The accuracy requirements for CTs are specified in IEC 61869-2 [6]. For protection CTs (Class P), standard burdens and power factors are specified in Table II.

TABLE II
CLASS P CT STANDARD BURDENS (IEC 61869-2)

Burden (VA)	Power Factor
2.5	1
5.0	0.8 lagging
10	
15	
30	

The angle error limits for protection CTs are given in Table III.

TABLE III
PROTECTION CT ANGLE ERROR LIMITS (IEC 61869-2)

Class	Angle Error Limit (minutes)
5P and 5PR	±60
10P and 10PR	Not specified

A plot of angle error limit versus current is shown in Fig. 10.

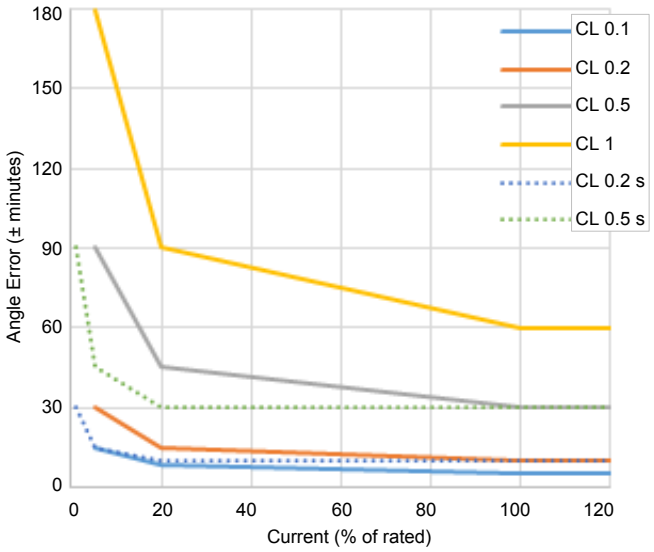

Fig. 10. Metering CT Angle Error Limits (IEC 61869-2)

The standard also specifies Class 3 and Class 5 accuracy classes. However, angle error limits are not specified for these. Accuracy limits are not specified above the rated burden or below 25 percent of the rated burden.

IEC 61869-3 specifies the accuracy requirements for VTs [7]. These are listed in Table IV and Table V. The requirements are specified at the rated frequency and for voltages ranging from 80 to 120 percent of the rated voltage. The requirements are also specified for a range of 0 to 100 percent of the rated burden for a power factor of 1 and a range of 25 to 100 percent of the rated burden for a lagging power factor of 0.8. Standard burdens are 25, 50, and 100 VA.

TABLE IV
METERING VT ANGLE ERROR LIMITS (IEC 61869-3)

Class	Angle Error Limit (minutes)
0.1	±5
0.2	±10
0.5	±20
1.0	±40
3.0	Not specified

TABLE V
PROTECTION VT ANGLE ERROR LIMITS (IEC 61869-3)

Class	Angle Error Limit (minutes)
3P	±120
6P	±240

B. Instrument Transformer Testing

Test sets are now available that allow angle errors to be measured to an accuracy of less than 3 minutes. These units run tests to determine the parameters to model the CT according to both ANSI IEEE and IEC standards. Table VI shows the results from a CT test performed by the authors. The angle errors are reported at various levels of secondary current and connected burden.

TABLE VI
EXAMPLE CT TEST RESULTS

Connected Burden (VA / PF)	Phase Displacement in Minutes at % Rated Current					
	1	5	10	20	50	100
200 / 0.5	2.63	0.83	0.42	0.21	0.06	0.04
100 / 0.5	2.75	1.02	0.64	0.39	0.21	0.13
50 / 0.5	2.80	1.11	0.77	0.52	0.31	0.22
25 / 0.5	2.75	1.15	0.83	0.59	0.37	0.27

The test results in Table VI are from a dual-rated generator CT that has both protection and metering specifications. These results show that CT angle accuracy can, in fact, be much better than the requirements of the standards.

C. Impact of Connected Burden

In general, manufacturers design instrument transformers to meet the previously described limits over a range of connected burdens, which includes the rated burden. The lowest errors do not necessarily occur when the connected burden matches the rated burden (either in impedance or power factor). If accuracy measurements are available from the manufacturer at various burdens or if test data are available (see Section III, Subsection B), the error for the actual connected burden can be estimated using the equivalent circuit shown in Fig. 5. However, this level of detail is often unavailable to the protection engineer.

Note that the transient performance of a CT during an external fault is also a function of the connected burden. A lower connected burden produces a better transient performance. It is therefore good practice to minimize the burden. However, this may not be optimal for motoring protection. We can see this in the test results shown in Table VI. For example, looking at the 10 percent rated current column, we see a phase displacement of 0.83 minutes at a 25 VA burden and a phase displacement of 0.42 minutes at a 200 VA burden. The angle error increases as the connected burden decreases. However, for this particular CT, the increase (0.41 minutes) is insubstantial.

IV. COMPARISON OF ANALOG AND MICROPROCESSOR-BASED RELAYS

Prior to the development of microprocessor-based generator relays, motoring protection was provided by electromechanical or solid-state relays. This section highlights some of the differences in these relay technologies relative to motoring protection.

A. Comparison Testing

Three different reverse power relays intended for generator motoring protection were tested in a laboratory to determine their relative performance under conditions that may occur during an inadvertent motoring event. The first relay was an electromechanical, two-and-a-half element (three phase

currents and two phase-to-phase voltages) relay (EM32R). The second relay was an analog, solid-state, three element (three phase currents and three phase-to-neutral voltages) relay (SS32R). The third relay was a microprocessor-based multifunction generator protection relay using a three element algorithm (μP32R).

An example application with the parameters listed in Table VII was used to set and calibrate the relays. Note that the sample EM32R relay had a nominal 120 V rating [8], the sample SS32R relay had a nominal 208 V rating [9], and the μP32R relay had a nominal rating of 20 V to 440 V [10]. A different VTR was used for calculating the secondary current and voltage injection values for the SS32R relay to ensure that it was in its best measuring range.

TABLE VII
EXAMPLE APPLICATION PARAMETERS

Parameter	Value
Rated apparent power	672 MVA
Rated power factor	0.9
Rated active power	605 MW
Rated voltage	22 kV
Actual motoring power	0.5% (–3.025 MW)
CTR	4,400 turns
Rated nominal current (secondary)	4.01 A
VTR	200 turns
Rated nominal voltage (secondary)	110 V
SS32R VTR	115 turns
SS32R rated nominal voltage (secondary)	191.3 V

All three relays were configured with a set point of 0.25 percent (50 percent of the machine's actual motoring power) using the appropriate CTR and VTR for the test relay. Then, test points for volt-ampere reactive (VAR) loading at various pre-motoring event power factors were calculated assuming that the unit was operating at the rated active power output before the motoring event. These test points were calculated using the simplifying assumption that the pre- and post-event VAR outputs did not change. Table VIII lists the pre-event power factor and VAR loading.

The current was set to provide the level of apparent power flow shown in Table VIII at the generator nominal voltage with the angle at 89 degrees resulting in a power flow in Quadrant 1 of the PQ plane, or –89 degrees resulting in a power flow in Quadrant 4 of the PQ plane. The current angle was then slowly ramped toward Quadrant 2 or Quadrant 3 until the relay tripped. The results are shown in Fig. 11. Note that the P-axis is scaled to one-tenth of the Q-axis to make the data easier to see.

TABLE VIII
PRE-EVENT POWER FACTOR AND VAR LOADING

Pre-Event Power Factor	VAR Loading (MVAR)
0.900 lagging	293.1
0.950 lagging	198.8
0.990 lagging	86.2
0.995 lagging	60.7
0.999 lagging	27.0
1.000	0
0.999 leading	–27.0
0.995 leading	–60.7
0.990 leading	–86.2
0.950 leading	–198.8
0.900 leading	–293.1

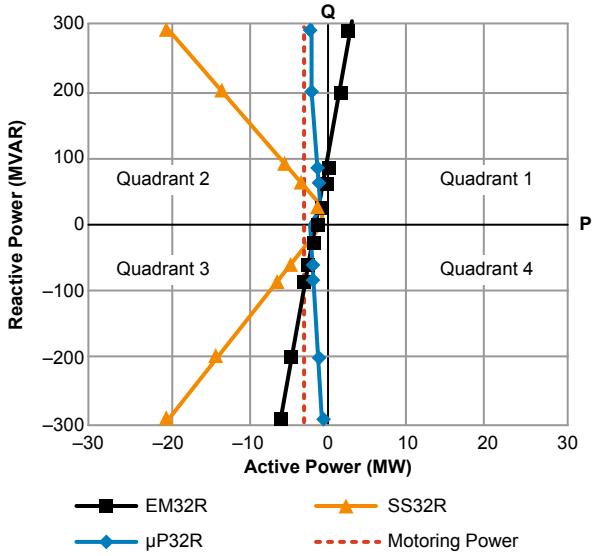

Fig. 11. Comparison of Three Motoring Protection Relays (primary PQ plane)

The following are some observations made from the data. The reader is cautioned to consider that these results and observations are from a sample of only one of each type of relay.

A general observation is that all three relays tripped at nearly the exact same point for cases when the power factor was 0.999 (relatively low current flow). These trip points display a tilt in the tripping characteristic, showing increased sensitivity in Quadrant 2 versus Quadrant 3. Because all three relays showed this tilt, it may have been a common error in the ability of the test set to reproduce the correct angle at this extremely low current level (161 mA).

1) EM32R Relay

The tripping characteristic of the electromechanical relay appears to be fairly linear across the range of VAR loading tested. However, the maximum torque angle appears to be off, resulting in a definite tilt of the characteristic in the PQ plane. The relay's instruction manual was carefully examined for calibration instructions, but no guidance was given to check or calibrate the maximum torque angle of the device [8]. The user is instructed to calibrate the relay at unity power factor only. If the relay protecting a generator has a tilt in the maximum torque angle, it could be overly sensitive in one quadrant of the PQ plane and fail to trip in the other quadrant. Because the manual does not recommend checking the calibration of the maximum torque angle, it is unlikely that this condition would be identified during initial or routine tests.

2) SS32R Relay

The tripping characteristic of the analog, solid-state relay exhibits a large reduction in sensitivity as the VAR loading increases. Examination of the relay instruction manual reveals a caution that the relay is not suitable for applications where the power factor can be below 0.10 relative to the set point [9]. A power factor of 0.10 equates to a pre-event VAR loading of only 15.2 MVAR in this example application. It is believed that this limitation is caused by the analog circuitry having a linear range of only 0 to 10 times the set point. If the current is above 10 times the measuring circuit's calibration point (the apparent power is 10 times the active power), the circuit starts saturating (clipping), resulting in increased error and a large reduction in sensitivity. This relay would likely work dependably during sequential tripping conditions but fail to trip during an inadvertent motoring event.

3) μP32R Relay

The tripping characteristic of the microprocessor-based relay is fairly linear and perpendicular to the P-axis. While there is some variation in the line, in no case did the relay trip in the forward power direction. And, more importantly, with the 50 percent margin applied, there was no case where it crossed the actual motoring power line resulting in a dependability failure.

4) Recommendation

Based on these tests, the authors recommend that relays used for inadvertent motoring event protection be tested at apparent power levels representative of at least the leading and lagging reactive power outputs expected at the unit's rated power factor during initial and periodic testing. This may reveal whether the relay's reverse power tripping characteristic is suitable to detect an inadvertent motoring event and properly initiate tripping. However, this precaution does not address errors introduced by the instrument transformers—it only addresses the relay's measuring circuit.

B. Advantages of Microprocessor Technology

Several advancements have been made in microprocessor-based designs that have a direct bearing on performance. Microprocessor-based designs, unlike many electromechanical and solid-state relays, typically carry out three-phase calculations using either the two- or three-wattmeter method (depending on the VT connection). The benefits are twofold. First, a three-phase calculation remains accurate in the event that the voltages or currents are unbalanced during motoring. Second, by using measurements from all phases of the voltage and current, the three-phase calculation tends to average out the errors inherent in the individual phases. This is illustrated in Fig. 12. Here, currents and voltages are injected into a hardware platform (described in Section VI). Single-phase and three-phase power calculations are performed, and the results are compared with the injected power in order to calculate accuracy. Note that the three-phase measurement is slightly closer to the true value (1 per unit [pu]) and has less variation than the individual single-phase measurements.

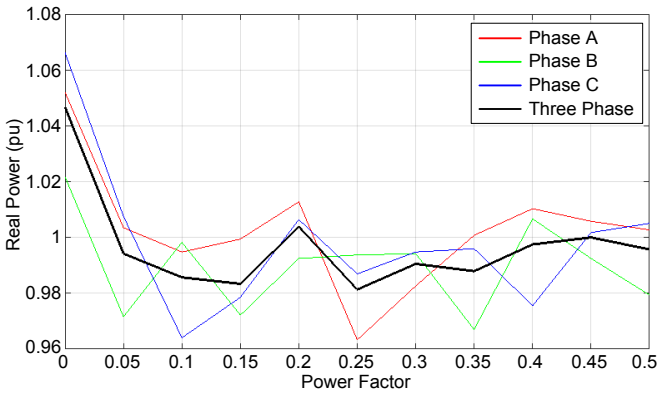

Fig. 12. Comparison of Single-Phase and Three-Phase Measurements

Another benefit of a microprocessor-based implementation is filtering. In general, mechanical power translates directly to active power at the fundamental frequency. Microprocessor-based algorithms calculate power from phasor quantities. In addition, these relays track frequency to ensure that the phasors are accurate when the frequency deviates from nominal. On the other hand, analog devices, such as product-type induction cylinder relays, are affected by off-nominal frequency and harmonics [11]. In practice, however, this has not been known to be a significant problem.

Microprocessor-based relays typically have a very large dynamic range for current measurement. This means that they can accurately measure very small currents at unity power factor and can also remain accurate for the larger currents expected when reactive power is high. Finally, microprocessor-based relays are immune to drift.

Despite these improvements in microprocessor-based digital relays, they are still dependent on the instrument transformers. Because generator digital relays often have the disadvantage of using protection-class CTs, potentially resulting in greater error (whereas metering CTs could be used for the discrete legacy relay), there is a need for a new algorithm.

V. New Algorithm

This paper now introduces a new algorithm that incorporates a bias into the conventional reverse power characteristic as shown in Fig. 13. The new characteristic modifies the reverse power tripping characteristic. Instead of being at a fixed active power level at ±90 degrees on the PQ plane, a small angle bias is added so that the farther from the origin on the PQ plane the operating point becomes (where the angle error has an effect), the more relaxed the reverse power threshold becomes. Referring back to Fig. 1, with the modified characteristic, the measured operating point with the error would still be well inside the new tripping characteristic and the motoring protection would trip dependably. The bias angle should be greater than the largest expected angle error.

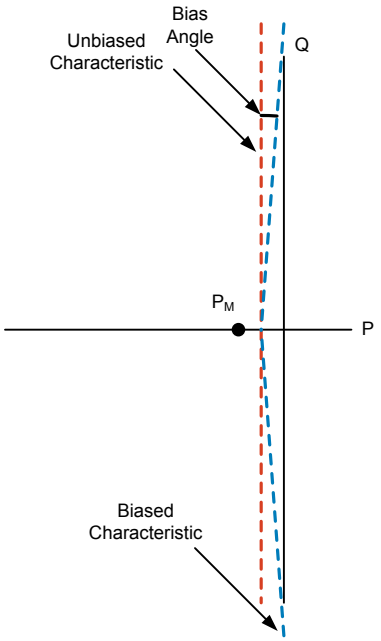

Fig. 13. Element Characteristic

There is no valid operating condition in which the machine would be operating at low forward power and high reactive power output where the dependability bias would cause a misoperation during normal operation, except possibly immediately following synchronization. If the generator is synchronized to the system with a fairly large difference between the generator terminal voltage and the system voltage, the reactive power flow upon initial synchronization could jump up quickly before the machine is loaded.

To address this condition, the element is adaptive. It starts out with the traditional fixed power threshold and then switches to the dependability-biased characteristic after a short delay. The logic works as follows. When the current is less than approximately 5 percent of generator-rated current for approximately 60 seconds, the element switches to the unbiased characteristic. At low current magnitudes, any angle error has little effect and the dependability-biased characteristic is not required. Once the current is greater than 5 percent for approximately 60 seconds, the element switches to the biased characteristic.

This adaptive characteristic makes the element more secure when starting and more dependable when shutting down. The delays prevent the element from chattering during a power swing. The element characteristic is therefore dynamic, a feature which is becoming more common in digital protection designs. Fig. 14 shows the scheme logic.

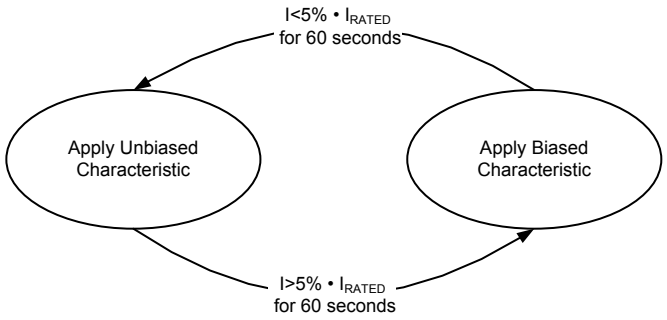

Fig. 14. Characteristic Switching Logic

A. Comparison With Low Forward Power

In the past, a low forward power scheme was applied in cases where the dependability of the reverse power element was marginal either because the relay is not sensitive at very low currents (as described in Section I) or because of angle errors at near-zero power factor. In this scheme, the power pickup threshold is shifted to the right-hand side (positive P) of the PQ plane. The element is blocked when the generator is offline because P is zero. Also, the element removal of the block must be delayed following synchronization to allow enough time for the generator power output to be ramped above the pickup threshold of the power element. The advantage of the scheme is that the pickup of the power element can be moved far enough into the positive power region to ensure pickup during an actual inadvertent motoring event. The drawback of the scheme is the reliance on the breaker status to enable and disable the scheme. In addition, a separate reverse power element is also required for the sequential tripping scheme.

The new dependability-biased characteristic provides the same level of dependability without the reliance on breaker status. The same element can be used for sequential tripping and for detection of inadvertent motoring.

B. Application Guidelines

The dependability-biased characteristic should be enabled when all of the following are true:

- Motoring power is low (less than 5 percent).
- VARs during inadvertent motoring can be significant (the AVR is not in power factor regulation mode).
- Angle errors are significant or not known (metering accuracy CTs are not used for the 32R protection).

A pickup threshold is selected according to typical guidelines (for example, 0.5 P_M). The default bias angle of 2 degrees is adequate for most applications. If the CT and VT angle accuracies are known (see Section III, Subsection A) then the bias angle can be set equal to the highest value. This preserves the pickup margin of the element.

VI. Algorithm Implementation

Generally, the process of designing, coding, testing, and releasing an enhancement to a protective relay is laborious and time-consuming. For this development, prior to implementation in a relay, the new algorithm was implemented on a real-time automation controller of the type used in utility applications. This approach allows the algorithm to be quickly tested and debugged in the hardware. Also, it allows the controller to be deployed in the field in a monitoring mode. This validates the algorithm under real-world conditions. Any issues arising during field trials can be quickly addressed.

The automation controller selected for this implementation has the following capabilities, which are essential for usage as a protection test platform:

- CT and VT measurements. These are performed by the CT/VT module, which includes multiple CT and VT inputs with conversion ranges of 0 to 22 A and 5 to 400 V L-N, respectively.
- All inputs are synchronously sampled and filtered to provide both root-mean-square (rms) values as well as phasor values over a frequency range of 45 to 65 Hz. Over this frequency range, the accuracy is typically ±1 percent for fundamental current and voltage quantities and ±0.1 percent for rms current and voltage quantities.
- Advanced logic and math functions. The logic engine of the controller supports the IEC 61131 programming languages, providing the flexibility to write custom function blocks with various user settings to account for multiple use cases. The logic engine supports math operations permitting active and reactive power to be calculated from complex voltage and current phasors.
- High-speed, deterministic performance. The controller has the ability to process logic at a fixed rate of 1 ms. Deterministic performance is maintained for all local and remote modules (analog as well as digital I/O). Additionally, the module records waveform oscillography up to 24 kHz and generates IEEE C37.118 synchrophasors.

The voltage and current signals are sampled and filtered in the CT/VT module before being sent to the automation controller module. The first step to implement the algorithm is to calculate three-phase active (3PD) and apparent (3SD) power, in this case using the two-wattmeter method (with open-delta VTs). These are shown in (7) and (8).

$$\begin{aligned} 3PD = {} & |VAB| \bullet |IA| \bullet \cos(\angle VAB - \angle IA) \\ & + |VCB| \bullet |IC| \bullet \cos(\angle VCB - \angle IC) \end{aligned} \tag{7}$$

$$3SD = |VAB| \bullet |IA| + |VCB| \bullet |IC| \tag{8}$$

The equation for the dependability-biased characteristic is (9).

$$BIASED\_PKP = PKP + 3SD \bullet \tan(ANGLE) \tag{9}$$

In (9), PKP is the pickup setting and ANGLE is the angle of the dependability-biased characteristic measured from the ordinate axis. For an ANGLE setting of 0 degrees, tan(0°) = 0, and the BIASED_PKP is equal to PKP for all values of apparent power.

The equation to check the operation of the element is (10).

$$OP = 3P < BIASED\_PKP \tag{10}$$

Fig. 15 shows the coding of the new function.

```
VAR_INPUT
Static : BOOL; //Setting to select threshold type dynamic or fixed
PU : REAL; //Setting for Reverse Power Pick Up Value in VA range from -100 VA to 100 VA in steps of 0.01 VA
PTCON : BOOL; //Setting to select connection type either WYE or Delta
P_Dynamic : REAL; //Setting to select dynamic or static threshold
Rev_PU_tim: REAL; //Setting to select Pick-Up Time (2000 msec for testing)
REV_RST_tim : REAL; //Setting to select Reset Time (3000 msec for testing)
Proc_Int : REAL; //Setting for processing interval (10 msec for testing)
P_Thresh : REAL; //Setting for Threshold Value
Py: REAL; // Real Power Value for Wye Connection
Sy : REAL;// Apparent Power Value for Wye Connection
PD : REAL; // Real Power Value for Delta Connection
SD : REAL; // Apparent Power Value for Delta Connection
```

```
IF PTCON THEN // PTCON variables define the connection type selected by the user.
P_Dynamic := PU+Sy*TAN(0.0349); // IF PTCON is True then user selected a WYE Connection. The angle is in radians (2°/57.3 = 0.0349)
ELSIF NOT PTCON THEN
P_Dynamic := PU+SD*TAN(0.0349); // IF PTCON is True then user selected a Delta Connection. The angle is in radians (2°/57.3 = 0.0349)
END_IF


IF Static THEN
P_Thresh := PU; //For test case static Value will be 69*0.0125 =(0.865), where 69 is the voltage and 0.0125 is the minimum current
ELSIF NOT Static THEN
P_Thresh := P_Dynamic;
END_IF
```

Fig. 15. IEC 61131 Structured Text Implementation of Controller Logic

VII. Testing and Results

The controller logic was simulated and debugged with a relay secondary injection test set in a laboratory environment as shown in Fig. 16. Testing of the logic by injecting various current values at different power factors provided the first verification of the accuracy of the system.

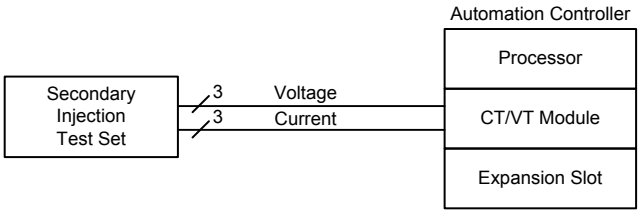

Fig. 16. Setup for Secondary Injection Testing of Automation Controller

The plot in Fig. 17 shows that the basic power measurement accuracy of the controller is quite good.

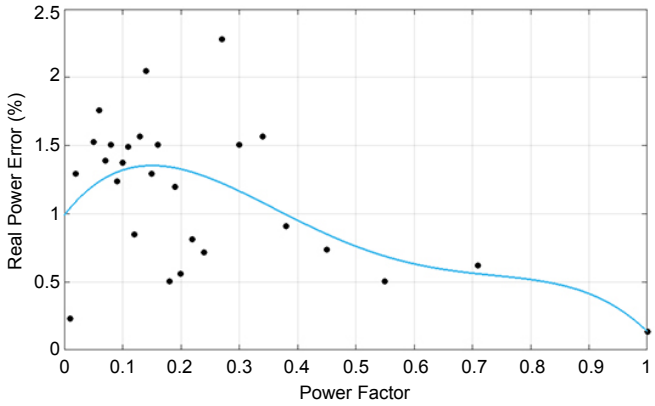

Fig. 17. Test Results of Active Power Error as Function of Power Factor

The algorithm prototype implemented in the automation controller is presently installed in monitoring mode on two turbine generators. However, real-world results were not available at the time of this writing.

VIII. Conclusion

This paper describes how the dependability of the reverse power element in detecting an inadvertent motoring condition can be compromised on machines with low motoring power. It also presents a new algorithm with a dynamic operating characteristic. The concept can be categorized with other dynamic characteristics; for example, the memory-polarized mho, which expands to provide better resistive coverage, or the adaptive percentage-differential, which increases its slope during periods when CT saturation is more likely.

The new scheme is very simple to understand and use. The exact setting for the dependability bias angle is not critical, so default settings can be applied in most applications. The adaptive element introduces no significant reduction in the security of the protection. So, the authors recommend the use of this element in all applications to reduce the possibility of failure to trip when the rare inadvertent motoring event occurs.

The scheme was implemented on an automation controller. This approach demonstrates the effectiveness of such a hardware platform in the development of novel protection functions.

Test data from several example reverse power relays reveal that the first step in determining the answer to the question posed by this paper (generator motoring protection—are you protected?) is to test relays under realistic conditions that would occur during an inadvertent motoring event. However, this simple measure is still not enough to account for other angle errors that may be present in the complete protection system. The improved protection characteristic presented in this paper can make the protection system tolerant of all known or unknown errors.

IX. References

[1] M. Thompson and D. Finney, "Antimotoring Protection With Dependability-Biased Characteristic," proceedings of the 13th International Conference on Developments in Power System Protection, Edinburgh, United Kingdom, March 2016.

[2] IEEE Standard C37.102, IEEE Guide for AC Generator Protection.

[3] R. V. McGrath, N. A. Izquierdo, and G. J. Wirth, "Reverse-Power Relay Response Under High-VAR Unit Conditions," proceedings of the 53rd Annual American Power Conference, Chicago, IL, April 1991.

[4] D. Riemert, *Protective Relaying for Power Generation Systems*. CRC Press, Boca Raton, FL, 2006.

[5] IEEE Standard C57.13, IEEE Standard Requirements for Instrument Transformers.

[6] IEC 61869-2, Instrument Transformers – Part 2: Additional Requirements for Current Transformers, 2012.

[7] IEC 61869-3, Instrument Transformers – Part 3: Additional Requirements for Inductive Voltage Transformers, 2011.

[8] Polyphase Power Directional Relay for Anti-Motoring Protection, Type GGP53C Instruction Manual. Available: http://www.gegridsolutions.com.

[9] BE1-32R, BE1-32O/U, Directional Power Relay Instruction Manual. Available: http://www.basler.com.

[10] SEL-700G Instruction Manual. Available: https://www.selinc.com.

[11] W. A. Elmore, S. E. Zocholl, and C. A. Kramer, "Effect of Waveform Distortion on Protective Relays," *IEEE Transactions on Industry Applications*, Vol. 29, No. 2, February 1993, pp. 404–411.

X. Biographies

Dale Finney received his bachelor of engineering degree from Lakehead University and his master of engineering degree from the University of Toronto. He began his career with Ontario Hydro, where he worked as a protection and control engineer. Currently, Dale is employed as a senior power engineer with Schweitzer Engineering Laboratories, Inc. His areas of interest include generator protection, line protection, and substation automation. Dale holds several patents and has authored more than 20 papers in the area of power system protection. He is a member of the main committee and the rotating machinery subcommittee of the IEEE PSRC. He is a senior member of the IEEE and a registered professional engineer in the province of Nova Scotia.

Michael J. Thompson received his B.S., magna cum laude, from Bradley University in 1981 and an M.B.A. from Eastern Illinois University in 1991. Upon graduating, he served nearly 15 years at Central Illinois Public Service (now AMEREN), where he worked in distribution and substation field engineering before taking over responsibility for system protection engineering. Prior to joining Schweitzer Engineering Laboratories, Inc. (SEL) in 2001, he was involved in the development of several numerical protective relays while working at Basler Electric. He is presently a Fellow Engineer at SEL Engineering Services, Inc. He is a senior member of the IEEE, main committee member of the IEEE PES Power System Relaying Committee, and past chairman of the Substation Protection Subcommittee of the PSRC. Michael is a registered professional engineer in six jurisdictions, has published numerous technical papers, and holds a number of patents associated with power system protection and control.

Normann Fischer received a Higher Diploma in Technology, with honors, from Technikon Witwatersrand, Johannesburg, South Africa, in 1988; a BSEE, with honors, from the University of Cape Town in 1993; an M.S.E.E. from the University of Idaho in 2005; and a Ph.D. from the University of Idaho in 2014. He joined Eskom as a protection technician in 1984 and was a senior design engineer in the Eskom protection design department for three years. He then joined IST Energy as a senior design engineer in 1996. In 1999, Normann joined Schweitzer Engineering Laboratories, Inc., where he is currently a fellow engineer in the research and development division. He was a registered professional engineer in South Africa and a member of the South African Institute of Electrical Engineers. He is currently a senior member of the IEEE and a member of the American Society for Engineering Education (ASEE).

Amandeep Kalra is an automation systems engineer with Schweitzer Engineering Laboratories, Inc. (SEL) in Lynnwood, Washington, with several years of experience in designing automation systems and communications networks. He has authored numerous technical papers focusing on IEC 61131-based automation controllers, Ethernet networks, and Ethernet-based communications protocols as well as IEC 61850 communications standards. He has represented SEL at various international conferences and IEC 61850 interoperability demonstrations organized by UCA and frequently teaches engineering design and application of IEC 61850 solutions. He has a bachelor of technology degree in instrumentation and control engineering from the National Institute of Technology, India, and a master's degree in electrical engineering from California State University, Northridge.